DBpia

論文 95-12-12-35

Ultra-high Speed Photodetector using a-Ge:H Thin Film Photoconductor for Picosecond Optical Signal at 0.8μm Wavelength

Kyoo Nam Choi* Regular Member

수소화된 박막 Ge을 이용한 0.8μm 파장 피코초대 광신호용 초고속 수광소자

正會員 崔 圭 南*

ABSTRACT

Hydrogenated amorphous germanium photoconductors which respond to picosecond light signal have been fabricated using magnetron sputtering method. These photoconductors have been characterized measuring the spectral response, the responsivity, the photoconductivity, and the photoresponse to the picosecond light pulse. The mobility lifetime product of $1.2\times10^{-14}cm^2/V$ has been estimated from the measured photoconductance, and also the carrier lifetime of 30 psec has been estimated from the photoresponse to the incident picosecond light pulse.

要 約

마그네트론 스퍼터링 방법으로 증착된 수소화된 비정질 저메니움 박막반도체를 사용하여 피코(10-12)초대의 광신호에 응답할 수 있는 광도전성수광소자를 제작하였다. 파장별 빛에대한 응답성, 광전변환효율, 광도전율, 피코초대의 광신호에 대한 응답을 측정하여 이 수광소자의 특성을 분석하여 보았다. 측정된 광도전율로 부터 수광소자내 케리어의 기동성과 수명시간의 곱($\mu\tau$)은 $1.2\times10^{-14}cm^2/V$ 임을 알 수 있었고, 피코초대의 광펄스를 이용한 응답특성 측정결과로 부터 이 수광소자의 케리어 수명시간은 30 psec 임을 알수 있었다.

* 시립인천전문대학 통신과
論文番號 : 95347-1007
接受日字 : 1995年 10月 7日

www.dbpia.co.kr

Ⅰ. Introduction

Continued advances in novel semiconductor material using molecular beam epitaxy and microfabrication techniques have led to the fabrication of extremely fast photodetectors for visible and infrared wavelengths with modulation bandwidths in excess of multi-gigahertz and speeds of response in the picosecond region. We can expect that subpicosecond electronic devices will soon be available.

One the other hand, a new class of high-speed devices has emerged which use photoconductors for electrical pulse generators, sampling gates, high-voltage switches, and other applications in addition to their traditional use for light detection. The ability to generate and detect electronic waveforms with picosecond precision has led to the development of a complete picosecond electronic instrumentation capability for the characterization of high-speed materials and devices. Unlike detectors, the optical pulses are used in this case as a precise clock to control the generation and detection of electronic events, with virtually no time jitter.

In high speed optical local area networks (LAN) application, the photodetectors that have good responsivity at a wavelength of 0.85 μm and picosecond pulse durations are needed for integrated optical waveguide devices. The current difficult process of butt coupling of discrete crystalline silicon photodetectors to integrated optical waveguides can be replaced by depositing a thin semiconductor material onto the waveguides and photolithographically fabricating integrated photodetectors. Although the hydrogenated amorphous silicon (a-Si:H) photodiodes can be fast in response speed, the spectral response decreases rapidly for wavelengths beyond 0.7 μm. However the bandgap of hydrogenated amorphous germanium (a-Ge:H) is lower than that of a-Si:H, and thus it can improve the longer wavelength response. Also the bandgap of a-Ge:H can be tailored by adjusting the hydrogen content [1]. It is more difficult to prepare the electronically high quality a-Ge:H films in comparison with those of a-Si:H because of weak Ge:H bonds and large sticking coefficient of Ge related radicals [2]. The various methods of depositing a-Ge:H films were attempted such as ion beam sputtering [3], ECR plasma deposition [2], sputtering [4], magnetron sputtering [5], chemical vapor deposition [6], and diode rf glow discharge deposition [7].

In this paper, the magnetron sputtering method is used to deposit a-Ge:H photoconductive films having ultra-short relaxation time in picosecond range due to its low impurity level during deposition, followed by post deposition optical annealing to remove shallow defects.

Ⅱ. Picosecond Photoconductivity

A typical example of a picosecond photoconductor is shown in Fig.1. This photoconductor consists of a thin photoconducting film on an insulating substrate on which metal electrodes have been deposited in the configuration of a microstrip transmission line. A picosecond light pulse is focused on the active region of the photoconductor, which consists of a narrow gap between two microstrip electrodes. The analysis of the photoconducting gap can be represented by time-varying macroscopic circuit elements by neglecting retardation effects caused by the radiating currents and charges in the gap, if the dimensions of the

www.dbpia.co.kr

gap and the transmission line cross section are small relative to the distance an electromagnetic signal travels in the shortest time interval of interest.

Following this approach, the photoconductor is represented which is the sum of dark conductivity Go and time-varying photoconductance g(t), in parallel with a capacitance Cg imbedded in a transmission line. The time varying conductance term can be derived from the rate of dissipation of electrical energy in the photoconductor as

$$g(t) = \frac{1}{V_g^2} \int (n \cdot e \cdot \eta_n + p \cdot e \cdot \eta_p) |E|^2 dxdydz, \quad (1)$$

where V_g is the bias voltage across the gap, n and p are carriers, e is the electronic charge, n and p are electron and hole mobilities and

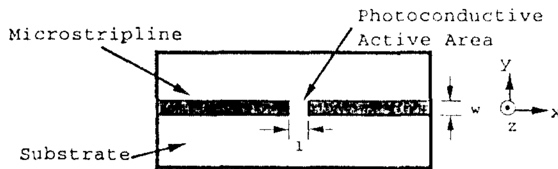

(a) Upper view of photoconductor.

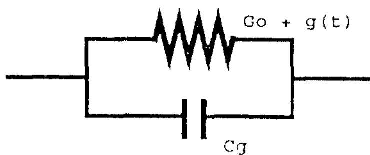

(b) Equivalent circuit model of active area.

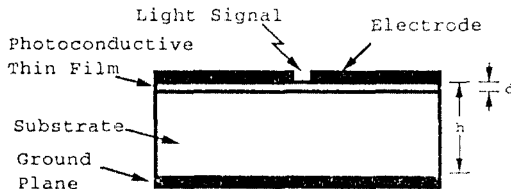

(c) Cross-sectional view of thin film photoconductor.

Fig. 1. Schematic diagram of a thin film photoconductor.

E is the electric field. Assuming an uniform electric field, $E(x) = V_g/l$, when the optical illumination is very low ($G_o \gg g$), the initial carrier density at $t = 0^+$ is denoted as

$$n = p = \frac{(1-R) \cdot \alpha\epsilon(x, y) \cdot \exp^{-\alpha z}}{h\nu}, \quad (2)$$

where R is the reflectance, is the optical absorption constant, ϵ is the incident optical pulse energy per unit area. Accordingly the initial photoconductance can be expressed as

$$g(t = 0^+) = (1-R) \frac{e}{h\nu} \frac{\mu_n + \mu_p}{l^2} W_p \quad (3)$$

if all of the incident light is focused and absorbed, where Wp is the total energy of the incident optical pulse. A lower limit for the mobility of the minority carrier can be calculated using this equation. However the time evolution of photoexcited electrons and holes may differ due to different capture rates by defect sites. Also the distribution of photoexcited carriers may not be uniform inside the photoconductive gap in the high optical injection regime ($G_o \ll g$) so that a space charge field develops. In picosecond photoconductivity, the characteristic time is one of the important parameters which explains this effect. The characteristic time (dielectric relaxation time τ_d) for the relaxation of the field is a complicated function of the geometry and the illumination condition. Assuming the spatial average of the macroscopic circuit parameters of conductance and capacitance, the dielectric relaxation time can be expressed as

$$\tau_d = \frac{\epsilon(x, y, z, t)}{\sigma(x, y, z, t)} \simeq \frac{C_g}{g} = \frac{|E|^2 dxdydz}{|E|^2 dxdydz}. \quad (4)$$

where ϵ is the dielectric constant. This τ_d can vary from nanoseconds for low excitation to

www.dbpia.co.kr

picoseconds for very large excitation. However, in the case of millimeter wave applications, the assumption of a time-invariant capacitor is no longer valid and the real part of the ϵ may be time varying.

Ⅲ. Materials for Picosecond Photoconductors

The absorption of a photon and the subsequent generation of an electron-hole pair inside the semiconductor is an intrinsically fast process, being limited by the uncertainty principle and the requirement that the frequency spectrum of the optical pulse fall within the absorption bands. The time for the electronic transition from bound to free state can, in principle, be as short as one optical cycle, and subsequently does not limit the rise time of the photocurrent. However the subsequent evolution of the photocurrent following excitation by a very short optical pulse is influenced by many factors, such as mobility transient and recombination, which is usually a much slower process and produces a long-lasting trailing waveform. An effective method of reducing the free-carrier lifetime to reduce the above trailing waveform can be achieved by introducing a moderate density of defects into the semiconductor which act as traps and recombination centers. The capture time τ_c can be estimated from

$$\tau_c = \frac{1}{N_t \cdot A_c \cdot \langle v_{th} \rangle} \tag{5}$$

where N_t is the trap density, A_c is the capture cross section and $\langle V_{th} \rangle$ is the mean thermal velocity. This defect density can be introduced by radiation damage and impurities or the use of polycrystalline/amorphous semiconductor materials. The use of high defect densities to produce short carrier lifetime causes the substantial reduction in quantum efficiency and carrier mobilities due to increased elastic scattering from the defects.

The formation of good ohmic contacts in high-defect density semiconductors is another task in fabrication of picosecond photoconductors, because non-ohmic contacts along with an internal electrostatic field results in a photovoltaic response in addition to a photoconductive signal. Fortunately metallic contacts on semiconductors with moderate to high defect densities tend to exhibit ohmic behavior due to short depletion layers which permit efficient tunneling currents to pass through the contacts. The use of annealing for fabricating amorphous picosecond photoconductors to remove shallow defects, but retain deep traps having fast capture time and slow emission rates, is a useful technique for improving the mobility without loss of response speed.

Ⅳ. Thin Film a-Ge:H Photodetector Fabrication

Amorphous hydrogenated germanium (a-Ge:H) is a suitable material for infrared detection due to smaller bandgap than amorphous hydrogenated silicon (a-Si:H) or amorphous hydrogenated silicon-germanium alloy (a-SiGe:H). The hydrogen in this amorphous tetrahedrally coordinated semiconductor effectively reduces the density of defect related states in the pseudogap, thus this is particularly useful for the film deposition method having an inherently high density of defects. However the effectiveness of hydrogen in defect compensation of amorphous germanium is much less than that of silicon. It is gener-

www.dbpia.co.kr

ally accepted that the photoconductive response of a-Ge:H is several orders of magnitude lower than that of a-Si:H. A set of criteria is established to judge material quality, such as the electron product and the ratio of photocurrent to dark current derived from photoconductivity. Also the spectral response of the material which is related to the bandgap is specified.

A photoconductor with low responsivity such as amorphous hydrogenated germanium usually suffers from high level of dark current. The reason for this is due to not only the inherent property of the material but also the relatively large geometry of the photoconductive gap in comparison with laser spot size, ~10 ㎛ diameter spot. This adverse effect was minimized by connecting a finger-like electrode, having 20 ㎛ width, to the active area. This electrode pattern was printed on the emulsion glass mask plate with opaque background. The shape of the photoconductor, which has broadband microstripline structure [8], is shown in Fig. 2.

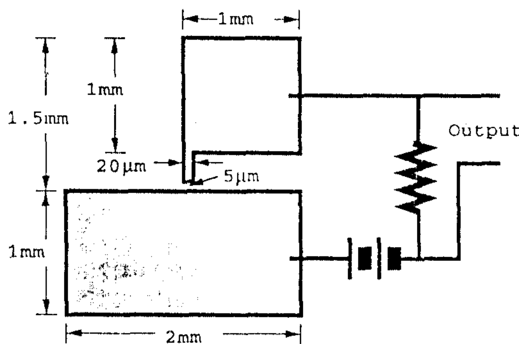

Fig. 2. The geometry of a-Ge:H photoconductor.

A microscope slide glass was used as a substrate. The sample were deposited using a RF planar magnetron sputtering machine with a semi-insulating crystalline germanium target having 99.99% purity. The gas flows were maintained to 2.8 sccm of argon and 13.8 sccm of hydrogen resulting in 3 mTorr of total pressure after pumping to 5×10^{-6} Torr of base pressure. During deposition, the temperature of glass substrate was maintained to 150°C and the RF power was controlled to 40 W. The deposition rate was adjusted to ≈0.5 Å/sec until reaching 0.5㎛ of thickness. The post-deposition annealing was done at 250°C for 1 hour in 1×10^{-5} Torr vacuum to remove shallow defects, but retaining deep traps having fast capture time. The surface of the deposited a-Ge:H film, which is evaluated using a scanning electron microscope (SEM), is shown in Fig. 3.

Fig. 3. The surface of deposited a-Ge:H thin film taken by SEM.

www.dbpia.co.kr

After photolithography process using Karl Suss mask aligner, metallization was done by evaporating 1200 Å of aluminum and 2000 Å of gold by using the resistive heater evaporator followed by lift-off process. Ohmic contact was formed by sintering at 450°C for 2 minutes using the lamp heater in vacuum. This thin film semiconductor showed a tendency of post-deposition atmospheric pickup, forming Ge-O and C-H related layer, unless an immediate passivation layer was coated on. This adverse change will include the change of the infrared absorption spectrum and time-dependent changes of electronic properties. The antireflection coating (1160Å) using Si_3N_4 layer was done immediately after lift-off process by using the tungsten shadow mask to avoid the above adverse effects. The Si_3N_4 target was used with the parameters such as 1.9 sccm of nitrogen and 31 sccm of argon, total pressure of 15 Hg after achieving 2×10^{6} Torr of base pressure. The 400 W of RF power was used, and the refractive index of 1.82 was obtained when the sample was measured using an ellipsometer. The transmittance of this layer was measured as 95.4 % at 0.85μm wavelength.

V. Results

The first property measured was the spectral response as shown in Fig.4. This spectral response was measured by using a monochrometer and a xenon lamp. The bandgap of a-Ge:H can be tailored by adjusting the hydrogen contents during the film deposition process, and normally it varies from 0.9 μm to the cut-off wavelength of crystalline germanium. The light was chopped at 260 Hz, and the output voltage was measured by using a lock-in amplifier when a 10 V bias was applied to the a-Ge:H photoconductor. The measured response showed a 3 dB spectral wavelength-width of 0.4 μm (0.65μm~1.05 μm) having a peak at the wavelength of 0.87 μm.

The second property measured was the mobility-lifetime ($\mu\tau$) product. At this time, the photoconductivity was measured by chopping the light at 260 Hz using a lock-in amplifier to suppress the noise level. When 9 μW (3.85×10^{13} photons/sec) of average optical power was focused to a≈7 μm diameter spot, the measured current level from the lock-in

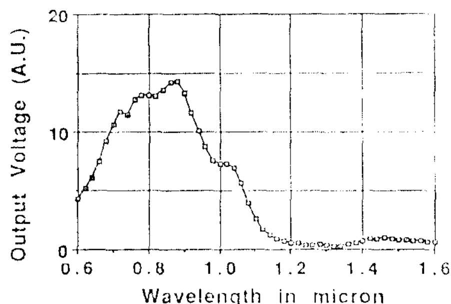

Fig. 4. Spectral response of a-Ge:H photoconductor

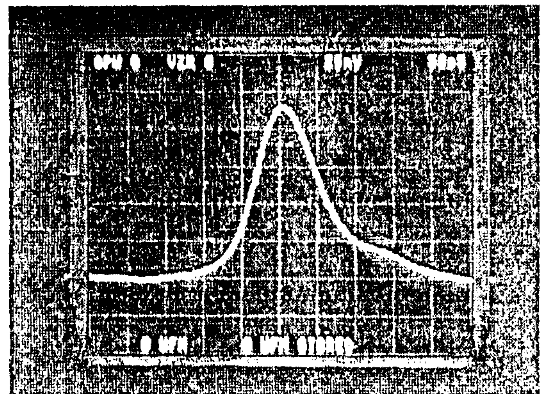

Fig. 5. Photoresponse of a-Ge:H photoconductor to the incident 100 ps FWHM light pulse.

www.dbpia.co.kr

amplifier was 0.4 nA at 10 V bias voltage with light on and 0.02 nA with light off. This is equivalent to a responsivity of 4.4×10^{-5} A/W, and a photoconductivity of $4.2 \times 10^{-8} (\Omega.cm)^{-1}$. From these values, we can estimate the mobility-lifetime product from the formula in [5] as

$$\mu\tau = \frac{\sigma_{ph} \cdot d}{I_o} = 1.2 \times 10^{-14} \frac{cm^2}{V} \qquad (6)$$

where d is the film thickness, e is the electron charge anf I_0 is the intensity of the light source.

The photosignal response was measured as shown in Fig.5. The light source in this measurement had the specification of 850 nm wavelength, 50 KHz repetition rate and optical energy of 10^{-9} J per pulse. The a-Ge:H photoconduotor with a 5μm photoconductive gap was biased at dc 10 V, and the signal was amplified using a wideband microwave amplifier having a 44 dB voltage gain. From the equation (3), we can derive the equation (7) for the estimation of mobility as

$$\mu = \frac{V_{out}}{R_L} \frac{hc/\lambda}{e} \frac{L_{gap}^2}{V_{bias}} \frac{1}{I_{pulse}} = 4.2 \times 10^{-4} \frac{cm^2}{V \cdot sec} \qquad (7)$$

where V_{out} is the output voltage before amplification, R_L is the load resistance, h is the Planck constant, c is the light speed, λ is the wavelength, L_{gap} is the photoconductive gap length, V_{bias} is the dc bias voltage and I_{pulse} is the optical energy per pulse. Thus the carrier lifetime can be estimated from (6) and (7) as 30 ps.

Ⅵ. Conclusions

In conclusion, we have prepared a hydrogenated amorphous germanium photoconductor in a broadband microstripline structure. The thin photoconductive active layers were grown by magnetron sputtering, followed by the optical annealing. We measured the spectral response, the responsivity, the photoconductivity, and the photoresponse to the picosecond light pulse, to characterize the fabricated photoconductors. The mobility lifetime product of $1.2 \times 10^{-14} cm^2/V$ has been estimated from the photoresponse to the incident picosecond light pulse at 0.85 μm wavelength, and also the carrier lifetime of 30 psec has been estimated from the photoresponse to the incident picosecond light pulse. The applications are foreseen in the area of ultra-high speed optical communication, electronic sampling gates, microwave generator, and microwave mixer, where both ultra-high speed and thin film semiconductor structure are necessary.

References

1. P. D. Persans et al, "Optical properties of a-Ge:H - structural disorder and H alloying," *Optical Effects in Amorphous Semiconductors, AIP Conf. Proc. No. 120, Snowbird Utah*, pp.349-355, 1984.
2. T. Aoki et al, "Hydrogen dilution effects on properties of ECR plasma deposited a-Ge:H," *J. Non-crystalline Solids*, Vol. 114, pp.798-800, 1989.
3. M. K. Bhan, L. K. Malhotra, and S. C. Kashyap, "Electrical, optical, and structural properties of reactive ion beam sputtered hydrogenated amorphous germanium films," *J. Appl. Phys.*, Vol. 65, No. 1, pp.241-247, Jan. 1989.
4. T. D. Moustakas and W. Paul, "Transport and recombination in sputtered hydrogenated amorphous germanium," *Phys. Rev. B*, Vol. 16, No. 4, pp.1564-1576, Aug. 1977.
5. R. A. Rudder, J. W. Cook and G. Lucovsky,

www.dbpia.co.kr

"High photoconductivity in magnetron sputtered amorphous hydrogenated germanium films," *Appl. Phys. Lett.*, Vol. 43, No. 9, pp.871-873, Nov. 1983.
6. D. R. Larson and R. J. Phelan, Jr., "Hydrogenated amorphous germanium detectors deposited onto channel waveguides," *Opt. Lett.*, Vol. 15, No. 10, May 1990.
7. W. A. Turner et al, "Structural, optical, and electrical characterization of improved amorphous hydrogenated germanium," *J. Appl. Phys.*, Vol. 67, No. 12, pp.7430-7438, Jun. 1990.
8. Kyoo Nam Choi, "Frequency response and CMRR enhancement of optical balanced receiver by using resonance in μ-wave frequency band," *5th Joint Conference on Com. & Inf.*, *Kyungju*, pp.105-108, Apr. 20-22 1995.

崔 圭 南(Kyoo Nam Choi) 정회원

1953년 8월 2일생
1976년 2월 : 서울대학교 공학사
1989년 12월 : 미국 Texas A&M 대학 전기공학과 공학석사
1992년 8월 : 미국 Texas A&M 대학 전기공학사 공학박사
1979년 5월~1987년 7월 : (주)대우
1992년 7월~1994년 8월 : 금성중앙연구소 책임연구원
1994년 8월~현재 : 시립인천전문대학 통신과 조교수
※주관심 분야 : 초고속광통신, 박막반도체소자

www.dbpia.co.kr